NUMERICAL METHODS FOR THE EVALUATION OF THE LÖWDIN α-FUNCTION

Nemanja SOVIC[1] and James D. TALMAN[2,*]

Department of Applied Mathematics and Centre for Chemical Physics, University of Western Ontario, London, Ontario, Canada N6A 5B7; e-mail: [1] nemanjasovic@hotmail.com, [2] jtalman@uwo.ca

Received January 10, 2005
Accepted April 26, 2005

This article is dedicated to Professor Josef Paldus, who has contributed so much to quantum chemistry.

The problem of expanding an angular momentum wave function centered at one point in terms of angular momentum wave functions centered at another point is analysed. The emphasis is on obtaining methods that can be applied to functions that are defined numerically, in contrast to analytic methods. Three numerical approaches are described, and it is found that one leads to extremely accurate results. The question of the rate of convergence of the resulting series is discussed, and results of the application of the expansion to the calculation of nuclear attraction three-center integrals, and electron–electron four-center integrals are presented.

Keywords: Gaussian; Orbitals; Slater orbital; Hartree–Fock; Wave function; Numerical methods; Quantum chemistry.

I. INTRODUCTION

All calculations of molecular electronic properties require the evaluation of so-called multicenter integrals. Without the possibility of obtaining these, essentially all calculations, from the simplest Hartree–Fock to the most complex many-body perturbation theory and coupled-cluster calculations, to which Prof. J. Paldus has made such definitive contributions, would be impossible. The basic multicenter integral problem is to evaluate matrix elements of angular momentum wave functions centered at the various nuclei in a molecule. The simplest such integrals are the overlap integrals of the form

$$I(\mathbf{R}) = \int g_{l'm'}(\mathbf{r} - \mathbf{R})^* f_{lm}(\mathbf{r})\, \mathrm{d}\mathbf{r}\,. \qquad (1)$$

Other, more complicated integrals are the nuclear attraction three-center integrals involving the matrix elements of the nuclear Coulomb potential

of one nucleus and angular momentum functions centered at two other nuclei and the electron–electron repulsion integrals involving products of four angular momentum wave functions.

The problem of obtaining these integrals is very simple if the functions are Gaussian type orbitals (GTOs) of the form

$$f_{lm}(\mathbf{r}) = r^l \exp(-\alpha r^2) C_{lm}(\hat{\mathbf{r}}) \tag{2}$$

where

$$C_{lm}(\theta,\phi) = \sqrt{\frac{4\pi}{2l+1}}\, Y_{lm}(\theta,\phi) \tag{3}$$

because of the essential property that the product of two such functions at different centers is a finite linear combination of such functions centered at an intermediate point. For this reason, the vast majority of quantum chemistry calculations employ Gaussian functions. While GTOs have been invaluable in myriad practical calculations, they are not a complete answer to the problems of computational chemistry since they cannot describe the behaviour of the electronic wave functions at the nuclei, and superpositions of large numbers of them are required to give accurate results. As well, variational optimisation of the radial factors is not very feasible.

Many calculations in atomic physics employ numerical orbitals defined on a radial mesh[1]. Such functions permit the application of the variational principle through the Hartree–Fock equation to obtain accurate results using much smaller sets of functions, as well as providing a better description of the electronic behaviour at the nuclei. However, with the exception of diatomics, numerical orbitals have not been extensively used in molecular calculations, although progress in this has been made by one of us[2].

The problems associated with using more general functions than GTOs can be partially solved if an angular momentum function centered at one point can be expanded in terms of angular momentum functions centered at another point. In principle, the completeness of the spherical harmonics suggests that the expansion

$$f_{lm}(\mathbf{r}-\mathbf{R}) = \sum_{LML'M'} F_{lLL'mMM'}(r,R)\, C_{LM}(\hat{\mathbf{r}})\, C_{L'M'}(\hat{\mathbf{R}}) \tag{4}$$

can be used for calculations involving orbitals centered at more than one point. The function $F_{lLL'mMM'}(r,R)$ is often called the Löwdin α-function[3]. It will be seen that the sum is singly infinite, in that $|L - L'| \le l$. Thus, for example, if the expansion is known for $g_{l'm'}(\mathbf{r} - \mathbf{R})$ in Eq. (*1*),

$$I(\mathbf{R}) = \frac{4\pi}{2l+1} \sum_{L'=|l-l'|}^{l+l'} \int_0^\infty G_{l'lL'm'mM'}(r,R) f_{lm}(r) r^2 \, \mathrm{d}r \, C_{L'M'}(\hat{\mathbf{R}}) \qquad (5)$$

from the orthogonality of the spherical harmonics.

In this note, a number of methods of computing the α-function numerically will be described. One of these, the Fourier transform method, has been used extensively in practical molecular calculations[2], but the more direct methods suggested below are probably more accurate and efficient.

II. ANALYTIC EXPRESSIONS

It is convenient to use the unnormalised harmonic functions defined in Eq. (*3*). We note two properties of the $C_{lm}(\hat{\mathbf{r}})$. The product of two such functions can be expanded in terms of Wigner 3–*j* coefficients as

$$C_{lm}(\theta,\phi) C_{l'm'}(\theta,\phi) = \sum_{LM} (-1)^M (2L+1) \begin{pmatrix} l & l' & L \\ 0 & 0 & 0 \end{pmatrix} \begin{pmatrix} l & l' & L \\ m & m' & -M \end{pmatrix} C_{LM}(\theta,\phi) \, . \quad (6)$$

The expansion of a plane wave in spherical harmonics is given by

$$\mathrm{e}^{\mathrm{i}\mathbf{k}\cdot\mathbf{r}} = \sum_{lm} \mathrm{i}^l (2l+1) j_l(kr) C_{lm}(\hat{\mathbf{k}})^* C_{lm}(\hat{\mathbf{r}}) \, . \qquad (7)$$

It is sufficient to obtain expressions for the α-function only for the case $l = 0$ since in the more general case $f_{lm}(\mathbf{r})$ can be factored:

$$f_{lm}(\mathbf{r}) = r^l f_0(r) C_{lm}(\hat{\mathbf{r}}). \qquad (8)$$

The function $r^l C_{lm}(\hat{\mathbf{r}})$ defines the solid harmonic

$$C_{lm}(\mathbf{r}) = r^l C_{lm}(\hat{\mathbf{r}}) \, . \qquad (9)$$

The terms in $k^l C_{lm}(\hat{\mathbf{k}})$ in the identity $\mathrm{e}^{\mathrm{i}\mathbf{k}\cdot(\mathbf{r}-\mathbf{R})} = \mathrm{e}^{\mathrm{i}\mathbf{k}\cdot\mathbf{r}} \mathrm{e}^{-\mathrm{i}\mathbf{k}\cdot\mathbf{R}}$ lead to the translation formula for solid harmonics

$$\begin{aligned} C_{lm}(\mathbf{r}-\mathbf{R}) = & \sum_{l_1 m_1 l_2 m_2} (-1)^{l_2+m} (2l_1+1)(2l_2+1) \times \\ & \times \frac{(2l+1)!!}{(2l_1+1)!!\,(2l_2+1)!!} \begin{pmatrix} l_1 & l_2 & l \\ 0 & 0 & 0 \end{pmatrix} \begin{pmatrix} l_1 & l_2 & l \\ m_1 & m_2 & -m \end{pmatrix} \times \\ & \times C_{l_1 m_1}(\mathbf{r}) C_{l_2 m_2}(\mathbf{R}) \, . \end{aligned} \qquad (10)$$

The sums are, however, constrained by $l_1 + l_2 = l$, $m_1 + m_2 = m$.

The spherically symmetric factor $f_0(r)$ in Eq. (*8*) can be expanded as

$$f_0(|\mathbf{r}-\mathbf{R}|) = \sum_{\lambda\mu} F_\lambda(r,R)\, C_{\lambda\mu}(\hat{\mathbf{r}})^*\, C_{\lambda\mu}(\hat{\mathbf{R}}) =$$

$$= \sum_{\lambda} F_\lambda(r,R) P_\lambda(\hat{\mathbf{r}}\cdot\hat{\mathbf{R}}) \qquad (11)$$

where

$$F_\lambda(r,R) = \frac{2\lambda+1}{2}\int_{-1}^{1} P_\lambda(t)\, f_0([R^2 - 2rRt + r^2]^{1/2})\, \mathrm{d}t\ . \qquad (12)$$

Equations (*10*) and (*11*) can be combined to give

$$f_{lm}(\mathbf{r}-\mathbf{R}) = \sum (-1)^{l_2+m}(2l_1+1)(2l_2+1)\frac{(2l+1)!!}{(2l_1+1)!!\,(2l_2+1)!!}\times$$

$$\times \begin{pmatrix} l & l_1 & l_2 \\ 0 & 0 & 0 \end{pmatrix}\begin{pmatrix} l_1 & l_2 & l \\ m_1 & m_2 & -m \end{pmatrix}\times$$

$$\times C_{\lambda\mu}(\hat{\mathbf{r}})^*\, C_{l_1 m_1}(\hat{\mathbf{r}})\, C_{\lambda\mu}(\hat{\mathbf{R}})\, C_{l_2 m_2}(\hat{\mathbf{R}})\, r^{l_1} R^{l_2} F_\lambda(r,R) =$$

$$= \sum (-1)^{l_2+m+\mu+M_1+M_2}(2l_1+1)(2l_2+1)(2L_1+1)(2L_2+1)\times$$

$$\times \frac{(2l+1)!!}{(2l_1+1)!!\,(2l_2+1)!!}\begin{pmatrix} l & l_1 & l_2 \\ 0 & 0 & 0 \end{pmatrix}\begin{pmatrix} l_1 & \lambda & L_1 \\ 0 & 0 & 0 \end{pmatrix}\begin{pmatrix} l_2 & \lambda & L_2 \\ 0 & 0 & 0 \end{pmatrix}\times$$

$$\times \begin{pmatrix} l_1 & l_2 & l \\ m_1 & m_2 & -m \end{pmatrix}\begin{pmatrix} l_1 & \lambda & L_1 \\ m_1 & -\mu & -M_1 \end{pmatrix}\begin{pmatrix} l_2 & \lambda & L_2 \\ m_2 & \mu & -M_2 \end{pmatrix}\times$$

$$\times C_{L_1 M_1}(\hat{\mathbf{r}})\, C_{L_2 M_2}(\hat{\mathbf{R}})\, r^{l_1} R^{l_2} F_\lambda(r,R)\ . \qquad (13)$$

The sum on the magnetic quantum numbers can be transformed in terms of a Racah 6–*j* coefficient:

$$\sum (-1)^{m+\mu+M_1+M_2} \begin{pmatrix} l_1 & l_2 & l \\ m_1 & m_2 & -m \end{pmatrix} \begin{pmatrix} l_1 & \lambda & L_1 \\ m_1 & -\mu & -M_1 \end{pmatrix} \begin{pmatrix} l_2 & \lambda & L_2 \\ m_2 & \mu & -M_2 \end{pmatrix} =$$

$$= (-1)^{l_1+l_2+\lambda+m} \begin{Bmatrix} l & L_1 & L_2 \\ \lambda & l_2 & l_1 \end{Bmatrix} \begin{pmatrix} l & L_1 & L_2 \\ -m & M_1 & M_2 \end{pmatrix} =$$

$$= (-1)^{l+\lambda+m} \frac{\Delta(l_1 l_2 l)\,\Delta(l_1 L_1 \lambda)\,\Delta(l_2 L_2 \lambda)\,\Delta(l L_1 L_2)}{(L_1 + l_1 - \lambda)!\,(L_2 + l_2 - \lambda)!\,(l_1 + \lambda - L_1)!\,(l_2 + \lambda - L_2)!} \times$$

$$\times \frac{(l + L_1 + L_2 + 1)!}{(L_1 + L_2 - l)!} \begin{pmatrix} l & L_1 & L_2 \\ -m & M_1 & M_2 \end{pmatrix} \tag{14}$$

where

$$\Delta(l_1 l_2 l) = \left[\frac{(l_1 + l_2 - l)!\,(l_2 + l - l_1)!\,(l + l_1 - l_2)!}{(l_1 + l_2 + l + 1)!} \right]^{1/2} . \tag{15}$$

Assembling the factors gives an expression for the α-function:

$$F_{l L_1 L_2 m M_1 M_2}(r,R) = \sum_{\lambda l_1} (-1)^{l_2+m} (2L_1 + 1)(2L_2 + 1) \begin{pmatrix} l \\ l_1 \end{pmatrix} \frac{q(L_1 \lambda; l_1)\, q(L_2 \lambda; l - l_1)}{q(L_1 L_2; l)} \times$$

$$\times \begin{pmatrix} l & L_1 & L_2 \\ 0 & 0 & 0 \end{pmatrix} \begin{pmatrix} l & L_1 & L_2 \\ -m & M_1 & M_2 \end{pmatrix} r^{l_1} R^{l-l_1} F_\lambda(r,R) \tag{16}$$

where

$$q(l l'; L) = \frac{(l + l' - L - 1)!!}{(l + l' + L + 1)!!} \begin{pmatrix} L \\ (L + l - l')/2 \end{pmatrix} . \tag{17}$$

In view of Eq. (*16*), it is sufficient for most purposes to limit the analysis to the $l = 0$ case. In order to assess the accuracy of various methods, the analytic result for the Slater type orbital (STO) case will be used. If

$$f_0(r) = \mathrm{e}^{-\alpha r} \tag{18}$$

$$F_\lambda(r,R) = \mathrm{i}\alpha r j_{\lambda+1}(\mathrm{i}\alpha r) h_\lambda^{(1)}(\mathrm{i}\alpha R) + \mathrm{i}\alpha R j_\lambda(\mathrm{i}\alpha r) h_{\lambda+1}^{(1)}(\mathrm{i}\alpha R) -$$

$$- (2\lambda+1) j_\lambda(\mathrm{i}\alpha r) h_\lambda^{(1)}(\mathrm{i}\alpha R) \qquad (19)$$

for $r \le R$, with a similar expression for $r \ge R$. The result for the more general STO $r^s \mathrm{e}^{-\alpha r}$ is readily obtained by differentiating s times with respect to α.

III. FOURIER TRANSFORM METHOD

It is well known that translation of a function in ordinary space corresponds to multiplication by a plane wave in momentum space. Explicitly, if

$$\tilde{f}(\mathbf{k}) = \int \mathrm{e}^{\mathrm{i}\mathbf{k}\cdot\mathbf{r}} f(\mathbf{r})\, \mathrm{d}\mathbf{r} \qquad (20)$$

then

$$f(\mathbf{r}-\mathbf{R}) = \frac{1}{(2\pi)^3} \int \mathrm{e}^{-\mathrm{i}\mathbf{k}\cdot\mathbf{r}} \mathrm{e}^{\mathrm{i}\mathbf{k}\cdot\mathbf{r}} \tilde{f}(\mathbf{k})\, \mathrm{d}\mathbf{k}\,. \qquad (21)$$

From Eq. (*7*), it follows immediately that if

$$f(\mathbf{r}) = f_{lm}(r) C_{lm}(\mathbf{r}) \qquad (22)$$

$$\tilde{f}(\mathbf{k}) = 4\pi \mathrm{i}^l C_{lm}(\mathbf{k}) \int_0^\infty j_l(kr) f_{lm}(r) r^2\, \mathrm{d}r$$

$$= 4\pi \mathrm{i}^l C_{lm}(\mathbf{k}) \tilde{f}_{lm}(k)\,. \qquad (23)$$

Therefore

$$f(\mathbf{r}-\mathbf{R}) = \frac{1}{2\pi^2} \sum_{LL'MM'} \mathrm{i}^{l-L+L'} (2L+1)(2L'+1) \int C_{LM}(\mathbf{k})^* C_{L'M'}(\mathbf{k})^* C_{lm}(\mathbf{k})\, \mathrm{d}\Omega_{\mathbf{k}} \times$$

$$\times C_{LM}(\mathbf{r}) C_{L'M'}(\mathbf{R}) \int_0^\infty j_L(kr) j_{L'}(kR) \tilde{f}_{lm}(k) k^2\, \mathrm{d}k =$$

$$= \frac{2}{\pi} \sum_{LL'MM'} \mathrm{i}^{l-L+L'} (2L+1)(2L'+1)(-1)^m \begin{pmatrix} l & L & L' \\ 0 & 0 & 0 \end{pmatrix} \begin{pmatrix} l & L & L' \\ -m & M & M' \end{pmatrix} \times$$

$$\times C_{LM}(\mathbf{r}) C_{L'M'}(\mathbf{R}) \int_0^\infty j_L(kr) j_{L'}(kR) \tilde{f}_{lm}(k) k^2\, \mathrm{d}k\,. \qquad (24)$$

Then $F_{lLL'mMM'}(r,R)$, as defined in Eq. (*4*), is given by

$$F_{lLL'mMM'}(r,R) = \mathrm{i}^{l-L+L'}(2L+1)(2L'+1)(-1)^m \begin{pmatrix} l & L & L' \\ 0 & 0 & 0 \end{pmatrix} \begin{pmatrix} l & L & L' \\ -m & M & M' \end{pmatrix} \times$$

$$\times \frac{2}{\pi} \int_0^\infty j_L(kr) j_{L'}(kR) \tilde{f}_{lm}(k) k^2 \, \mathrm{d}k \,. \qquad (25)$$

The numerical calculations of the spherical Hankel transforms of Eqs (*23*) and (*25*) present considerable difficulty because of the rapid oscillation of the integrand at large values of the transform variable. It has been shown[4] that this problem can be avoided by defining both the function and its transform on a logarithmic mesh. The problem is then reduced to making two successive Fourier transforms, which can be performed with an operation count proportional to $N \ln N$, where N is the number of mesh points. This method has been applied successfully in numerical molecular calculations for a number of small molecules[2].

A difficulty with the method is that the integrand decreases rather slowly, as k^{-4} at large k, in the case of *s*-wave functions with a cusp at the origin. This problem, which seems to be more serious in principle than in practice, can be partially obviated by subtracting from $f_{lm}(r)$ a Slater function with the same cusp behaviour and adding back the known analytic behaviour. A second slight drawback is that the numerical method requires using mesh values that are physically unrealistically small.

There is a very extensive literature on the application of Fourier transform methods to the multicenter integral problem. It was observed in 1962 by Prosser and Blanchard[5] that the two-center integral can be obtained as a convolution and hence in terms of Fourier transforms. This approach has been pursued extensively by Silverstone and co-workers[6], Steinborn and co-workers[7], and more recently by Safouhi and Hoggan[8].

IV. SERIES EXPANSIONS

Various authors[9–11] have obtained series expansions for the function $F_\lambda(r,R)$. The simplest of these is to rewrite Eq. (*12*) by introducing the variable $s^2 = R^2 - 2rRt + r^2$, $s\,\mathrm{d}s = -rR\,\mathrm{d}t$ as the integration variable:

$$F_\lambda(r,R) = \frac{2\lambda+1}{2rR} \int_{|r-R|}^{r+R} P_\lambda((r^2 + R^2 - s^2)/2rR) s f(s) \, \mathrm{d}s \,. \qquad (26)$$

The Legendre polynomial can be expanded using the binomial theorem to give an expansion for $F_\lambda(r,R)$:

$$F_\lambda(r,R) = (2\lambda+1)\sum_{kt} c_{\lambda kt}\left(\frac{r}{R}\right)^{2t+k-l} I_{2k+1} \tag{27}$$

where

$$c_{\lambda kt} = \sum_m \frac{(-1)^{m+k}(2\lambda-2m)!}{2^{2\lambda-2m+1}\, m!\,(\lambda-m)!\,(t-m)!\,k!\,(\lambda-m-t-k)!} \tag{28}$$

and

$$I_{2k+1} = (rR)^{-(k+1)}\int_{|r-R|}^{r+R} s^{2k+1} f(s)\,\mathrm{d}s\,. \tag{29}$$

This result is not useful in practice since the terms behave as $r^{-(\lambda+1)}$ for small r, whereas the result actually behaves as r^λ. There is therefore a drastic cancellation of large terms, even for small values of λ.

A more useful expansion can be obtained be making the change of variable $s = R + ry$, for $r < R$, in Eq. (*26*), as

$$F_\lambda(r,R) = \frac{2\lambda+1}{2}\int_{-1}^{1} P_\lambda\left(-y+\frac{r}{2R}(1-y^2)\right)\left(1+\frac{r}{R}y\right) f(R+ry)\,\mathrm{d}y =$$

$$= \frac{2\lambda+1}{2}\sum_{kpq}\frac{(-1)^{k+p+q}(2l-2k)!}{2^l\,k!\,(l-k)!\,p!\,q!\,(l-2k-p-q)!}\left(\frac{r}{2R}\right)^{l-2k-p}\times$$

$$\times\int_{-1}^{1} y^{p+2q}\left(1+\frac{r}{R}y\right) f(R+ry)\,\mathrm{d}y =$$

$$= \frac{2\lambda+1}{2^{2l}}\sum_{kpq}\frac{(-1)^{k+p+q}\,2^{2k+p}(2l-2k)!}{k!\,(l-k)!\,p!\,q!\,(l-2k-p-q)!}\left(\frac{r}{2R}\right)^{l-2k-p}\times$$

$$\times\left[J_{p+2q}+\frac{r}{R}J_{p+2q+1}\right] \tag{30}$$

where

$$J_n = \int_{-1}^{1} y^n f(R+ry)\,\mathrm{d}y\,. \tag{31}$$

This result can obviously be applied in the STO case to give an expression equivalent to that of Eq. (*19*). In the STO case

$$J_n = \frac{n!\, e^{-\alpha R}}{(\alpha r)^{n+1}} \left[e^{\alpha r} \sum_{p=0}^{n} \frac{(-\alpha r)^p}{p!} - e^{-\alpha r} \sum_{p=0}^{n} \frac{(\alpha r)^p}{p!} \right]. \qquad (32)$$

This expression manifests the difficulties that arise at small values of *r*. However, in this case the problem can be readily circumvented by rewriting the expression as

$$J_n = e^{-\alpha r} \sum_{p=0}^{\infty} \frac{n!}{(p+n+1)!} [(\alpha r)^p - (-\alpha r)^p]. \qquad (33)$$

V. NUMERICAL METHODS

The numerical calculation of the α-function evidently requires a minimum of the order of NL_{max} floating point operations (flops) where *N* is the number of mesh points, and L_{max} is the maximum *l* value required.

The most efficient method appears to be the use of the series of Eq. (*27*) for which the calculation of the integrals requires the evaluation of two indefinite integrals, each requiring ≈*N* operations. However, as noted above, this method appears to be impractical for small *r* and large *l* values.

The spherical Hankel transform approach of Eq. (*25*) requires ≈*N* ln *N* operations for each of two Fourier transforms, as well as the calculation of the $j_{L'}(kr)$. However, the transform $\tilde{f}(k)$ and the $j_{L'}(kr)$ are computed only once. Application of Eq. (*25*) avoids the use of Eq. (*16*) in the case $l > 0$.

One plausible approach to the problem is to evaluate the integral of Eq. (*12*) directly. This is probably best carried out using Gauss–Legendre integration giving the approximation

$$F_\lambda(r_i, R) = \sum_{j=1}^{N_{gl}} w_j P_\lambda(t_j)\, f_0([R^2 - 2r_i R t_j + r_i^2]^{1/2}) \qquad (34)$$

where w_j and t_j are the abscissas and weights for Gauss–Legendre integration. For each r_i and t_j, the function values can be interpolated independently of λ and the fixed values $P_\lambda(t_j)$ need be computed only once. This method then can be carried out very efficiently in $\approx NL_{max}N_{gl}$ operations.

A similar approach is to evaluate the integral of Eq. (*31*) numerically as

$$F_\lambda(r_i, R) = \sum_{j=1}^{N_{gl}} w_j P_\lambda\left(-t_j + \frac{r_i}{2R}(1 - t_j^2)\right)\left(1 + \frac{r_i}{R}\right) f_0(R + r_i t_j). \qquad (35)$$

This method is slightly less efficient than the previous one since the values of P_λ must be obtained afresh for each calculation. Since they satisfy a simple recurrence relation, this is not a major drawback, however.

VI. NUMERICAL RESULTS

In this section, numerical results will be presented for the three calculational methods described above. The calculations are made for the $l = 0$ Slater function $f(r) = e^{-r}$ and comparisons are made with the exact result of Eq. (*19*) for $R = 1.0$. The quantity calculated is

$$F_\lambda(r,R) = \frac{2}{\pi}\int_0^\infty j_\lambda(kr)\, j_\lambda(kR)\, \tilde{f}(k) k^2 \,\mathrm{d}k \qquad (36)$$

where

$$\tilde{f}(k) = \int_0^\infty j_0(kr)\, e^{-r} r^2 \,\mathrm{d}r\,. \qquad (37)$$

The calculations for the spherical Hankel transform approach are made on a mesh $[r_{min}, r_{max}]$ with mesh points uniformly spaced in the variable $\rho = \ln r$. The results for four cases are presented in Figs 1–4. In each case the error as a function of r is shown for $\lambda = 0$ and 10, and $r_{max} = 20.0$. The results for $r_{min} = 0.001$, for 128 mesh points ($\delta\rho = 0.0780$) are shown in Fig. 1, and for 256 mesh points ($\delta\rho = 0.0388$) are shown in Fig. 2. Corresponding

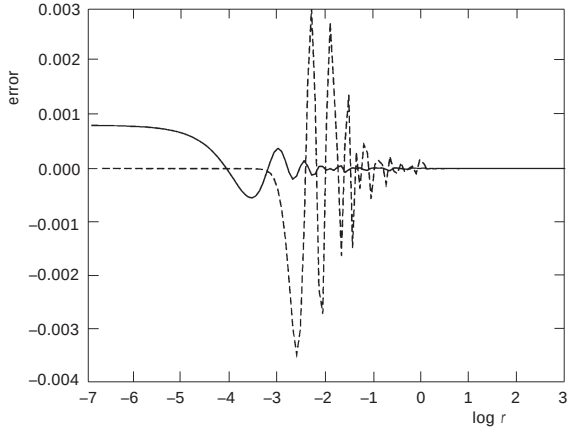

FIG. 1

Error in $F_\lambda(r,R)$, $R = 1$, defined in Eq. (*36*), as a function of $\rho = \ln r$, computed on 128 mesh points and $\rho_{min} = 0.001$. $\lambda = 0$ (——), 10 (– – –)

results with r_{min} = 0.00001, δρ = 0.0961 and 0.0478, respectively, are shown in Figs 3 and 4.

Evidently, the results for the smaller value of r_{min} are somewhat more accurate. This is because the integrand in the transform of $f(r)$ behaves like $r^{3/2}$ for $r \to 0$ so that values of r very close to the origin are required. Although the errors are fairly substantial, it should be observed that the result will occur in spatial integration and that the rapidly oscillating errors

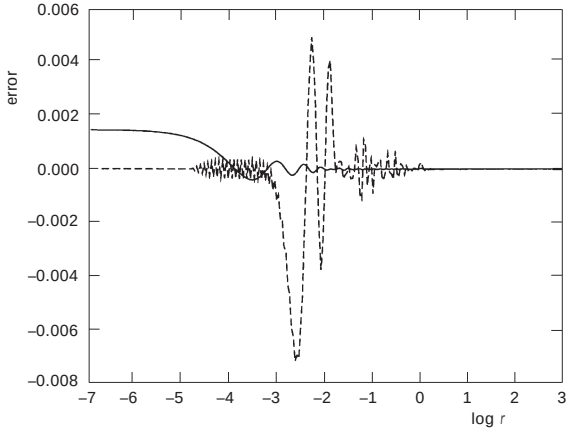

FIG. 2
As in Fig. 1, using 256 mesh points. λ = 0 (——), 10 (– – –)

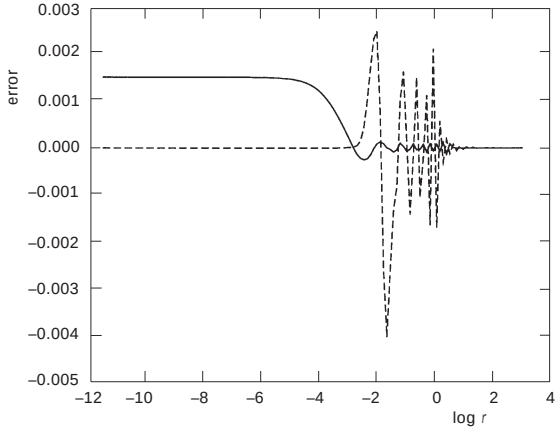

FIG. 3
As in Fig. 1, with ρ_{min} = 0.00001. λ = 0 (——), 10 (– – –)

may largely cancel. Moreover, the errors occur largely for $r < R$ and may be suppressed by the integration weight factor r^2. This point will be elaborated below.

Results using the numerical integration approach of Eq. (*34*), with $N_{gl} = 20$ are shown in Fig. 5, again for $\lambda = 0$ and 10. Clearly, the approximation is worst for r close to R and does not show the possibly compensating oscillating behaviour of the previous results. More detailed results are presented in

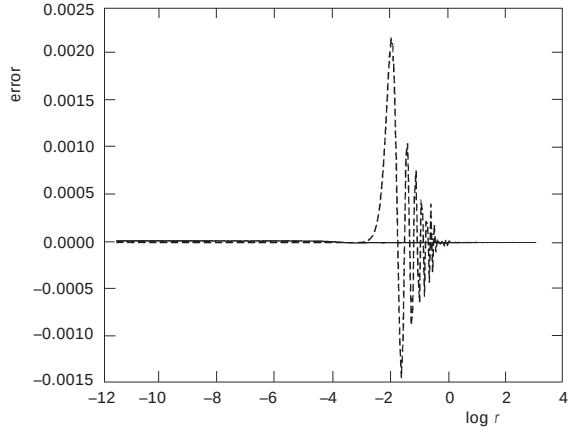

FIG. 4
As in Fig. 3, using 256 mesh points. $\lambda = 0$ (——), 10 (– – –)

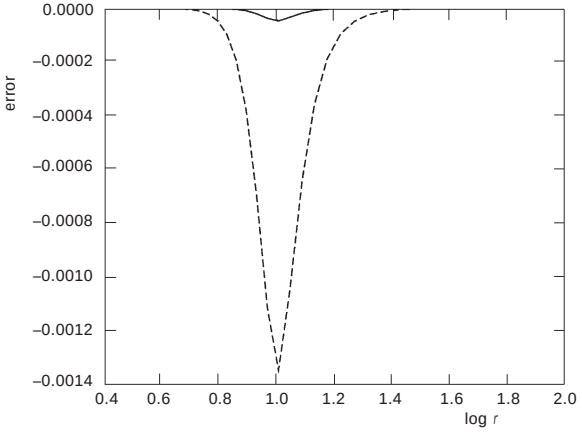

FIG. 5
Error in $F_\lambda(r,R)$, $R = 1$, defined in Eq. (*36*), as a function of $\rho = \ln r$, calculated using Eq. (*34*) and Gaussian integration on 20 mesh points. $\lambda = 0$ (——), 10 (– – –)

Table I, in which values of $F_\lambda(r,R)$, $R = 1.0$ are presented for $r = 0.9$, 1.0, and 1.1. The errors clearly decrease rapidly as $|R - r|$ increases, more or less independently of λ. The dependence of the error on N_{gl} is shown in Table II for $\lambda = 0$ and 10. These results indicate that the use of Eq. (*34*) does not offer significant improvement on the spherical Hankel transform approach.

The situation is markedly better using the approximation of Eq. (*35*). Indeed, it is found that for values of N_{gl} only slightly greater than λ, accuracy comparable to the machine accuracy 10^{-14} is obtained. The reason for this

TABLE I
Values of the function $F_\lambda(r,R)$ for $r = R = 1.0$, and the errors in using Eq. (*34*) for $r = 0.9$, 1.0, and 1.1, with $0 \le \lambda \le 20$. $N_{gl} = 40$

λ	$F_\lambda(1.0,1.0)$	δ_1	δ_2	δ_3
0	0.29700	–0.129E–07	–0.310E–05	–0.280E–07
1	0.24805	–0.389E–07	–0.931E–04	–0.847E–07
2	0.13367	–0.659E–07	–0.155E–04	–0.143E–06
3	0.07594	–0.945E–07	–0.218E–04	–0.205E–06
4	0.04760	–0.125E–06	–0.282E–04	–0.270E–06
5	0.03234	–0.159E–06	–0.346E–04	–0.341E–06
6	0.02333	–0.197E–06	–0.411–E04	–0.420E–06
7	0.01759	–0.240E–06	–0.478E–04	–0.507E–06
8	0.01373	–0.288E–06	–0.546E–04	–0.604E–06
9	0.01101	–0.343E–06	–0.615E–04	–0.714E–06
10	0.00903	–0.406E–06	–0.687E–04	–0.838E–06
11	0.00753	–0.479E–06	–0.761E–04	–0.980E–06
12	0.00638	–0.564E–06	–0.837E–04	–0.114E–05
13	0.00547	–0.661E–06	–0.915E–04	–0.133E–05
14	0.00474	–0.774E–06	–0.977E–04	–0.154E–05
15	0.00415	–0.905E–06	–0.108E–03	–0.178E–05
16	0.00367	–0.106E–05	–0.117E–03	–0.206E–05
17	0.00326	–0.123E–05	–0.126E–03	–0.238E–05
18	0.00292	–0.144E–05	–0.136E–03	–0.275E–05
19	0.00263	–0.168E–05	–0.146E–03	–0.317E–05
20	0.00238	–0.196E–05	–0.157E–03	–0.366E–05

TABLE II
The errors in $F_\lambda(1.0,1.0)$ for various values of N_{gl} using Eq. (*34*) for $\lambda = 0$ and 10

N_{gl}	$\lambda = 0$	$\lambda = 10$
6	0.750E–03	0.282E+00
8	0.335E–03	0.297E–01
10	0.178E–03	0.903E–02
12	0.105E–03	0.404E–02
14	0.675E–04	0.220E–02
16	0.458E–04	0.135E–02
18	0.325E–04	0.890E–03
20	0.239E–04	0.622E–03
22	0.181E–04	0.453E–03
24	0.140E–04	0.341E–03
26	0.111E–04	0.264E–03
28	0.890E–05	0.208E–03
30	0.726E–05	0.168E–03

TABLE III
The errors in $F_\lambda(1.0,1.0)$ for various values of λ using Eq. (*35*) with $N_{gl} = 20$

λ	Error	λ	Error
0	0.228E–14		
1	–0.111E–15	11	–0.801E–14
2	0.425E–14	12	–0.165E–16
3	0.643E–14	13	–0.125E–13
4	0.296E–14	14	–0.547E–14
5	0.239E–14	15	–0.904E–15
6	0.114E–13	16	–0.173E–13
7	–0.278E–14	17	–0.401E–14
8	0.294E–14	18	–0.581E–14
9	0.306E–14	19	–0.174E–12
10	–0.542E–14	20	–0.787E–11

is that the integration points are concentrated closer to the origin for t_j close to –1. Table III shows the error at $r = R = 1.0$ for $0 \le \lambda \le 20$ computed with $N_{gl} = 20$. These results are obtained using the computationally "exact" expression for the exponential function in Eq. (*35*). Since the interest in this investigation is in obtaining a numerical method, it is necessary to make a numerical interpolation on the function values, necessarily reducing the accuracy. Table IV shows the results corresponding to those of Table III if six-point interpolation is used to evaluate the function.

VII. CONVERGENCE ISSUES

The largest difficulty with the expansion using Eq. (*4*) may not be with the evaluation of the α-function, but with the slow convergence of the resulting series. Since the Slater function, which is representative of any physically realistic function, is not differentiable at the origin, the series is necessarily slowly convergent at **r** = **R**. In fact, it is not difficult to show from Eq. (*19*) that $F_\lambda(r,R)$ decreases as ρ^λ/λ^2, $\rho = \min(r,R)/\max(r,R)$ for large λ. For $r = R$, the terms decrease as λ^{-3}. This problem is exhibited in Fig. 6, which shows the difference between the approximation of Eq. (*4*) with $l_{max} = 20$ for **r** in the **R** direction, and the exact value, $e^{-|r-R|}$.

TABLE IV
Results as in Table III using six-point interpolation for the exponential function

λ	Error	λ	Error
0	0.687E–11		
1	0.286E–10	11	0.190E–10
2	–0.364E–10	12	–0.845E–11
3	–0.523E–11	13	–0.126E–10
4	–0.411E–11	14	0.522E–11
5	–0.948E–11	15	0.106E–10
6	0.123E–10	16	–0.201E–11
7	0.146E–10	17	–0.103E–10
8	–0.108E–10	18	0.170E–10
9	–0.107E–10	19	0.467E–11
10	0.604E–11	20	–0.239E–10

Figure 7 shows the related behaviour for $r = R$ as a function of the variable $\cos\theta = \mathbf{r}\cdot\mathbf{R}/rR$, again with $l_{max} = 20$. A further calculation shows that the rms percent error on integrating over space is 0.00367. This slow convergence calls into question the rationale for obtaining substantially greater accuracy in the numerical calculation.

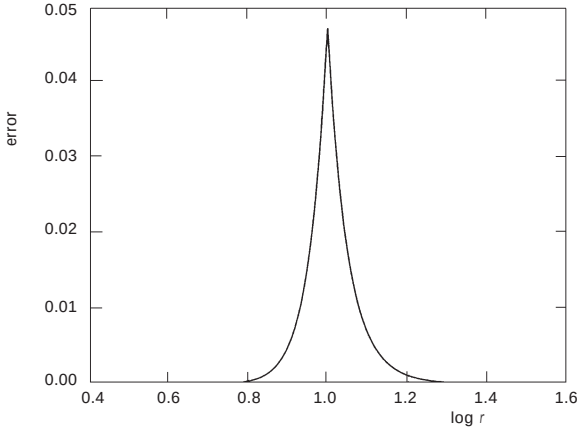

FIG. 6
The error (——) in $e^{-|r-R|}$, $R = 1$ when approximated by the expansion of Eq. (*4*), with $l_{max} = 20$

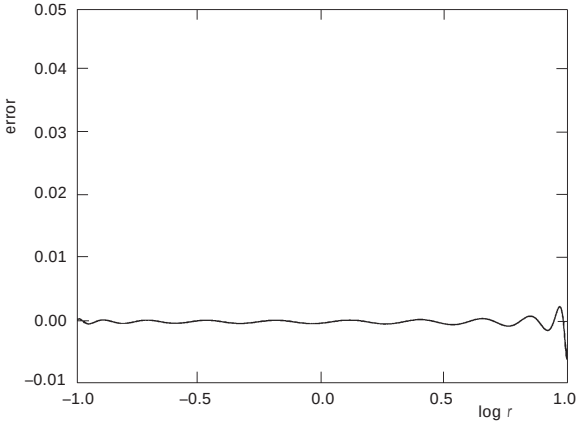

FIG. 7
The error (——) in $e^{-|\mathbf{r}-\mathbf{R}|}$, $|\mathbf{r}| = |\mathbf{R}| = 1$ as a function of $\cos\theta = \mathbf{r}\cdot\mathbf{R}/rR$ when approximated by the expansion of Eq. (*4*), with $l_{max} = 20$

On the other hand, the percent error, averaged over space, is 0.26×10^{-7}, showing the large extent to which the errors cancel. As well, in practice the expansion is multiplied by an orbital at another center, so that the percent error is largest where the integrand is relatively small.

To illustrate this, we consider the calculation of the three-centre nuclear attraction integral:

$$I = \int g(\mathbf{r} - \mathbf{a}_1)|\mathbf{r} - \mathbf{R}|^{-1} f(\mathbf{r} - \mathbf{a}_2)\, \mathrm{d}\mathbf{r} \qquad (38)$$

for $f(\mathbf{r}) = g(\mathbf{r}) = \mathrm{e}^{-r}$. The integral can be computed by expanding each of the three factors about an arbitrary centre and multiplying the resulting sums. The product of two such angular momentum sums is reduced to a single sum using the expansion Eq. (*6*). It can be shown that the convergence of the resulting series is geometric in the larger of the ratios r_1/r_2, r_2/r_3 where $r_1 \leq r_2 \leq r_3$ are the distances to the three centers. Evidently, the center should be chosen to minimise the larger of these two ratios, and this occurs when the ratios are equal, giving rise to a geometrical problem. The convergence is slowest in the case of an equilateral triangle, for which the ratio is $(\sqrt{5} - 1)/2 \approx 0.618$, the reciprocal of the golden mean.

TABLE V

The three-center nuclear attraction integral defined in Eq. (*38*) for the STO e^{-r} with $\mathbf{a}_1$ = (1,0,0), $\mathbf{a}_2$ = (0,1,0), $\mathbf{R}$ = (0,0,1) for various values of the angular momentum cut-off

l_{max}	Optimum center	Diagonal pade
0	0.1100573170	0.1001516687
2	0.1180530776	0.1187849700
4	0.1176524947	0.1176508027
6	0.1176893047	0.1176999547
8	0.1176920843	0.1176903565
10	0.1176903750	0.1176903259
12	0.1176906429	0.1176906552
14	0.1176906709	0.1176906222
16	0.1176906460	0.1176906325
18	0.1176906509	0.1176906299
20	0.1176906515	0.1176906306

Table V shows the result of this calculation for the case of the equilateral triangle $\mathbf{a}_1 = (1,0,0)$, $\mathbf{a}_2 = (0,1,0)$, $\mathbf{R} = (0,0,1)$ for various values of $l_{\max}$, the cut-off in the angular momentum sums. An alternative approach is to expand each orbital about the nucleus. The result is a single sum on l, which is however slowly convergent. A variety of nonlinear convergence acceleration techniques are available to improve the convergence rate. The result of computing the diagonal Pade approximant $[l_{\max}/2, l_{\max}/2]$ is also shown in Table V. In these results the main source of error is the radial integration. The results indicate that both approaches can give reliable results for modest values of $l_{\max}$.

VIII. FOUR-CENTER INTEGRALS

One of the most time-consuming processes in molecular calculations is the computation of the four-center integrals

$$I = \iint \chi_a(\mathbf{r}-\mathbf{R}_a)\,\chi_b(\mathbf{r}-\mathbf{R}_b)|\mathbf{r}-\mathbf{r}'|^{-1}\,\chi_c(\mathbf{r}'-\mathbf{R}_c)\,\chi_d(\mathbf{r}'-\mathbf{R}_d)\,\mathrm{d}\mathbf{r}\,\mathrm{d}\mathbf{r}' . \qquad (39)$$

The number of such integrals scales as $N^4/8$ and an efficient method for their calculation is essential. One approach to this problem[12] is to expand the products $\chi_a(\mathbf{r}-\mathbf{R}_a)\,\chi_b(\mathbf{r}-\mathbf{R}_b)$ about some center, perhaps $(\mathbf{R}_a + \mathbf{R}_b)/2$:

$$\chi_a(\mathbf{r}-\mathbf{R}_a)\,\chi_b(\mathbf{r}-\mathbf{R}_b) = \sum_{LL'MM'} P_{LL'MM'}(r,R)\,C_{LM}(\hat{\mathbf{r}})\,C_{L'M'}(\hat{\mathbf{R}}_m) . \qquad (40)$$

This product can be regarded as a charge density, and the integral as the interaction energy of two densities. The electrostatic interaction energy of two charge densities $\rho^{(1)}_{l'm'}(\mathbf{r}-\mathbf{R}_1)$, $\rho^{(2)}_{lm}(\mathbf{r}-\mathbf{R}_2)$, is given in momentum space by

$$E = \frac{1}{2\pi^2}\int \mathrm{e}^{\mathrm{i}\mathbf{k}\cdot\mathbf{R}}\,\tilde{\rho}^{(1)}_{l_1m_1}(\mathbf{k})\,\tilde{\rho}^{(2)}_{l_2m_2}(-\mathbf{k})\,\frac{1}{k^2}\,\mathrm{d}k \qquad (41)$$

where $\mathbf{R} = \mathbf{R}_1 - \mathbf{R}_2$. The four-center integrals can therefore be efficiently computed by storing the Fourier transforms of the "densities" in Eq. (*39*) and using Eq. (*41*) together with the expansion Eq. (*7*). Then

$$I = 32\pi\sum(-1)^{(l+L_1-L_2)/2+m}(2l+1)\begin{pmatrix} L_1 & L_2 & l \\ 0 & 0 & 0 \end{pmatrix}\begin{pmatrix} L_1 & L_2 & l \\ M_1 & M_2 & -m \end{pmatrix}\times$$

$$\times\, C_{lm}(\hat{\mathbf{R}})\,C_{L_1'M_1'}(\hat{\mathbf{R}}_{m_1})\,C_{L_2'M_2'}(\hat{\mathbf{R}}_{m_2})\int_0^\infty j_l(kR)\,\tilde{P}^{(1)}_{L_1L_1'M_1M_1'}(k)\,\tilde{P}^{(2)}_{L_2L_2'M_2M_2'}(k)\,\mathrm{d}k \qquad (42)$$

where the transforms $\tilde{P}^{(i)}$ are given by Eq. (*23*).

The values of the four-center integral for hydrogenic orbitals centered at the tetrahedral vertices $(a,a,a),(-a,-a,a),(-a,a,-a),(a,-a,-a)$, $a = 2/\sqrt{3}$ are shown in Table VI for various values of L_{max}, the maximum of L_1 and L_2 and l_{max}, the maximum of l, in Eq. (*42*). We also show the energy obtained for the CH_4 molecule in this geometry, in a minimal calculation using these orbitals and the Hartree–Fock atomic orbitals for C. The results show that mH accuracy is obtainable with only a modest calculational effort.

TABLE VI
The four-center integral I for hydrogenic orbitals at the four vertices of a tetrahedron at a distance 2.0 from its center. The energy for the CH_4 molecule is also shown

L_{max}	l_{max}	I	CH_4 energy
10	4	0.490985	–39.89240
12	4	0.490955	–39.89210
14	4	0.490945	–39.89200
16	4	0.490940	–39.89197
18	4	0.490938	–39.89195
20	4	0.490938	–39.89195
20	6	0.490915	–39.89147
20	8	0.490917	–39.89148

IX. DISCUSSION

The results presented show that the α-function can be efficiently calculated for numerically defined radial functions defined on arbitrary meshes. This opens the way not only for the calculation of multicenter integrals involving such functions, but also to further procedures such as the variational optimisation of such functions. Although the spherical Hankel transform method has been used successfully in the past, the numerical integration procedure defined in Eq. (*35*) is clearly more accurate and more efficient.

It is important to note, however, that the numerical Fourier Hankel transform method is essential to the calculation of the electron repulsion four-center integrals, as discussed briefly in Section VIII.

This research has been supported by the Natural Sciences and Engineering Research Council of Canada.

REFERENCES

1. Froese Fischer C.: *The Hartree–Fock Method for Atoms*. Wiley-Interscience, New York 1977.
2. a) Talman J. D.: *Phys. Rev. Lett.* **2000**, *84*, 855; b) Talman J. D.: *Int. J. Quantum Chem.* **2003**, *95*, 442.
3. Löwdin P.-O.: *Adv. Phys.* **1955**, *5*, 1.
4. a) Talman J. D.: *J. Comput. Phys.* **1978**, *29*, 35; b) Talman J. D.: *Comput. Phys. Commun.* **1983**, *30*, 93.
5. Prosser F. P., Blanchard C. H.: *J. Chem Phys.* **1962**, *36*, 1112.
6. For references, see: Antolovic D., Silverstone H. J.: *Int. J. Quantum. Chem.* **2004**, *100*, 146.
7. For a review, see: Grotendorst J.: *Ph.D. Thesis*. University of Regensburg.
8. For references, see: Safouhi H.: *Int. J. Quantum Chem.* **2004**, *100*, 172.
9. Sharma R. R.: *Phys. Rev. A: At., Mol., Opt. Phys.* **1981**, *13*, 517.
10. Silverstone H. J., Moats R. K.: *Phys. Rev. A: At., Mol., Opt. Phys.* **1977**, *16*, 1723.
11. Rashid M. A.: *J. Math. Phys.* **1981**, *22*, 271.
12. Talman J. D.: *J. Chem. Phys.* **1984**, *80*, 2000.